J Therm Spray Tech
https://doi.org/10.1007/s11666-022-01488-9

PEER REVIEWED

Energy Flux Characterisation of Atmospheric Pressure Plasma Spray Torches with Passive Thermal Probes

Kristian A. Reck[1] · Luka Hansen[1] · Maximilian Stummer[2] · Thorben Kewitz[3] · Holger Testrich[3] · Andreas Hinterer[2] · Rüdiger Foest[3] · Holger Kersten[1]

Submitted: 29 March 2022 / in revised form: 6 August 2022 / Accepted: 22 September 2022

Abstract Passive thermal probes were applied on two different plasma spraying devices to gain a detailed understanding of the energy flux towards the substrate under atmospheric pressure. The challenge of very high thermal load was solved by using an advanced time-resolved measuring and evaluation technique. The combination with a controlled movement of the jets allowed to obtain insightful radial profiles. The energy flux to the substrate changes linearly to the electrical input power. When adding diatomic gases (H_2/N_2) to the gas mixture the energy flux increases significantly, suggesting a more efficient energy transport. For increasing the axial distance, the energy flux shows a quadratic reduction. The obtained radial profiles are exemplarily utilized to show the inhomogeneous effect of powder injection on the energy flux distribution.

Keywords atmospheric plasma spray · calorimetric diagnostics · energy balance · spray plume diagnostics · thermal probes · thermal management

Abbreviations

A_S	Substrate area
P_{in}	Incoming power
J_{in}	Incoming power flux
T_S	Substrate temperature
C_S	Substrate heat capacity

✉ Kristian A. Reck
reck@physik.uni-kiel.de

[1] Institute of Experimental and Applied Physics, Kiel University, Kiel, Germany

[2] INOCON Technologie GmbH, R&D Coating Technology, Attnang-Puchheim, Austria

[3] Leibniz Institute for Plasma Science and Technology, Greifswald, Germany

Introduction

Plasma spraying is a well-established coating process for various coating materials and substrates. The high deposition rates and unique coating properties have led to a broad use in science and industry (Ref 1, 2). The areas of application range from thermal barrier coatings for energy-efficient turbines to wear and corrosion-resistant coatings as well as biocompatible layers in medicine (Ref 3-9).

Due to the strong dependence of coating properties on process parameters several diagnostic tools have been already used to study aspects of the plasma spray process in the past. Thus, diagnostics play an important role of process control and optimisation. The plasma itself or the effluent, respectively, have been analysed mainly by optical methods, e.g., optical emission spectroscopy, Rayleigh and Raman spectroscopy, schlieren imaging as well as computer tomography (Ref 10-14). The very high densities of an arc discharge and atmospheric pressure conditions prevent the application of established probe-based diagnostics like Langmuir probes or retarding field analysers. The only exception is enthalpy probes (Ref 15, 16) which are remotely related to the passive thermal probes present in this study. The usually injected powder particles have been studied with regard to their temperature and velocity distributions with high-speed cameras, pyrometers or electrical low-pressure impactors (Ref 17-19).

Selvan et al. (Ref 20) used numerical modelling to investigate the energy transfer to the substrate. Their results on the spatial distribution of energy flux and influence of gas flow and arc current are readily comparable to the

Published online: 09 November 2022

results obtained in this work directly because the plasma sources are very similar. The work of Hugot et al. (Ref 21) should be mentioned as well, as they measured the radial profile of energy flux as boundary conditions for their model on thermomechanical behaviour.

However, to the authors knowledge, there are no diagnostics already available which are capable of describing the interaction of the effluent and powder with the surface of a substrate during deposition. That issue is motivation for the application of passive thermal probes in this study. Passive thermal probes (PTPs) provide insight into the calorimetric interaction between the plasma and the particles and a surface (Ref 22, 23). The probe acts as a regular substrate while depositing, hence the results are directly useful for application-related uses. Via the change of temperature during a deposition process the energy flux can be deduced. This flux is composed of many contributions which among others are related to gas temperature, plasma properties as well as mass and temperature of the layer material.

More recent studies showed the applicability of PTPs in atmospheric pressure plasmas (Ref 24-28). This present study focuses on the results obtained with PTPs at two different atmospheric plasma spraying sources and on the necessary requirements and development in data processing. The results cover the variation of input power and the addition of molecular gases. Furthermore, several spatial measurements were performed and used for verification of a new time-resolved evaluation procedure.

When a substrate is located next to a plasma environment its temperature usually rises due to the higher energy density of a plasma compared to the surrounding. The energy transfer is a sum of several contributions and surface interactions. Figure 1 shows a schematic of a substrate energy balance (Ref 22). The main contributions during atmospheric plasma spraying are the following: (i) Fast particles, i.e., electrons, ions or neutrals, which impact on the substrate surface and deposit their kinetic energy P_{part}. (ii) Absorbed radiation P_{rad} which is composed of thermal radiation due to elevated temperatures and transitions of excited atoms and molecules. (iii) Due to the high flow of hot gas at atmospheric pressure, forced convection P_{conv} plays an important role when investigating plasma spraying. (iv) In the case of thermal plasma spraying the layer formation consists of macroscopic molten droplets. Their thermal energy and transition enthalpy P_{mat} can raise the substrate temperature as well. (v) The last main contribution stems from chemical reaction happening at the substrate surface P_{chem}. These can be exothermic reactions like conversion reactions or released binding energies during layer formation. Additionally, one has to mention the recombination of dissociated atoms, as molecular gases like hydrogen are regularly added to increase the energy flux (Ref 29).

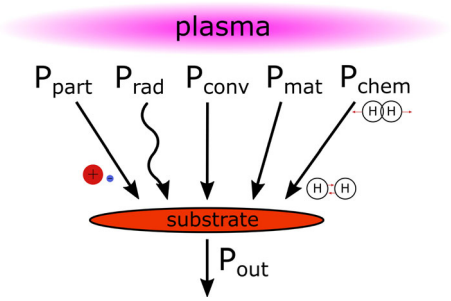

Fig. 1 Energy flux contributions of a plasma-substrate interaction

To measure the integral energy flux consisting of the mentioned contributions passive thermal probes (PTPs) as illustrated in Fig. 2 are used. A copper plate which acts as a substrate is spot-welded to a type K thermocouple and bias wire. This allows for an accurate and fast monitoring of the substrate temperature. Furthermore, no additional connection to the surrounding leads to a minimal thermal conduction. The steel shielding around the backside of the substrate plate ensures that no additional energy flux is collected. Thus, the only surface exposed to the plasma is the frontside of the copper plate. This well-defined area A_S allows for the normalisation of the incoming power P_{in} to an energy flux $J_{\text{in}} = P/A_S$ which will be discussed in section "Experimental Setup".

The results are focused on the applicability of passive thermal probes and the obtained insight into general, process-related dependencies to evaluate the possibilities and limits of this plasma diagnostic. The performed

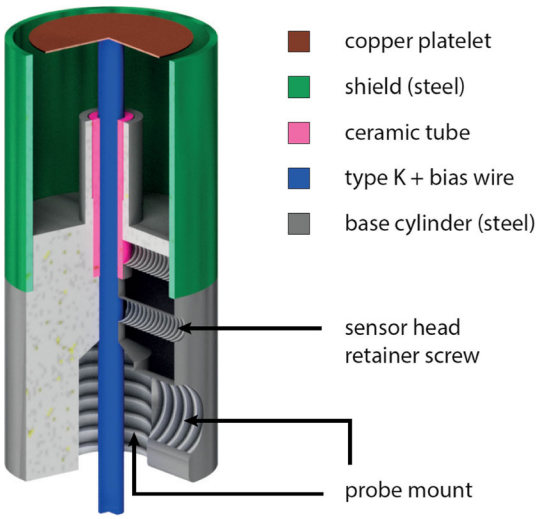

Fig. 2 Schematic layout of a passive thermal probe. Reprinted from Thin Solid Films, Vol. 669, Sven Gauter et al., Experimentally unraveling the energy flux originating from a DC magnetron sputtering source, pg. 8-18, Copyright (2019), with permission from Elsevier (Ref 30)

measurements were primarily done without a coating material (i.e., powder injection) to prevent the formation of a layer on the probe substrate which would change its heat capacity. However, some exemplary results with added powders are shown using the time-resolved evaluation method. In particular, the dependence of the energy flux on several discharge parameters of the plasma spraying devices will be discussed.

Experimental Setup

In order to measure the energy flux with a PTP, a specific sequence of different temporal temperature changes is needed as shown in Fig. 3. A single measurement starts with a heating phase when the probe is exposed to the plasma and its temperature increases rapidly followed by a subsequent cooling phase when the exposure is suppressed. This distinct change in probe temperature due to the energy flux can either be caused by turning the plasma on and off or by using a shutter (Ref 31). The time derivative of the substrate temperature T_S during the heating phase $T_{S,h}$ and during the cooling phase $T_{S,c}$ is used to calculate the energy influx

$$J_{in} = \frac{C_s}{A_s}\left(\dot{T}_{S,h} - \dot{T}_{S,c}\right)|T_{S,h} = T_{S,c}$$

with the heat capacity of the substrate C_S (Ref 27). The assumptions and derivation for that equation can be found in in previous studies (Ref 31, 32).

The adaption of this measuring principle to plasma spraying devices would make it necessary to turn the plasma on and off instantaneously as a shutter is not provided. However, a DC-jet usually experiences some fluctuation directly after start-up before it reaches a steady state. For that reason, the jet has to be started far off the probe until it has reached its final state.

Therefore, the start of the heating phase is realized by moving the jet at its maximum velocity of 500 mm/s to the probe position. Figure 4(a) shows the temporal change of temperature (dT/dt) over the substrate temperature. This way of depicting a temperature course like in Fig. 3 is a helpful tool for analysing the energy flux since the difference of temperature derivations in Eq. 1 can be directly deduced. The measuring procedure begins with the substrate at room temperature. When the jet gets closer the temperature rises, i.e., the derivation becomes positive. To ensure a constant energy flux the jet stops at the substrate position for defined time. Under this condition, the temperature change is almost constant. After the defined waiting time, in this example 0.5 s, the jet continues its movement and moves away from the substrate, thereby decreasing the energy flux. Without the energy flux from the jet, the energy loss induced by the temperature difference between substrate and environment becomes dominant. This leads to a decreasing substrate temperature, thus, a negative derivative until the room temperature is reached again.

This approach allows for the calculation of the energy flux by averaging over the time of constant energy flux. Because the idea of this method goes back to the dT-method in (Ref 32) it will be referred to as the established method.

The very high energy flux for certain experimental conditions, e.g., short distance or added molecular gases, results in temperatures that could damage the probe. The thermal load can be limited by reducing the stationery time but a duration of at least 0.5 s is needed for a reliable evaluation of the $T_S(t)$ curve. That is the incentive to modify the measuring approach for harsh plasma environments as for plasma spraying.

The change is rather simple but has heavy implications on the thermal load and the evaluation of the energy flux in general. Instead of resting the jet at the probe position, the

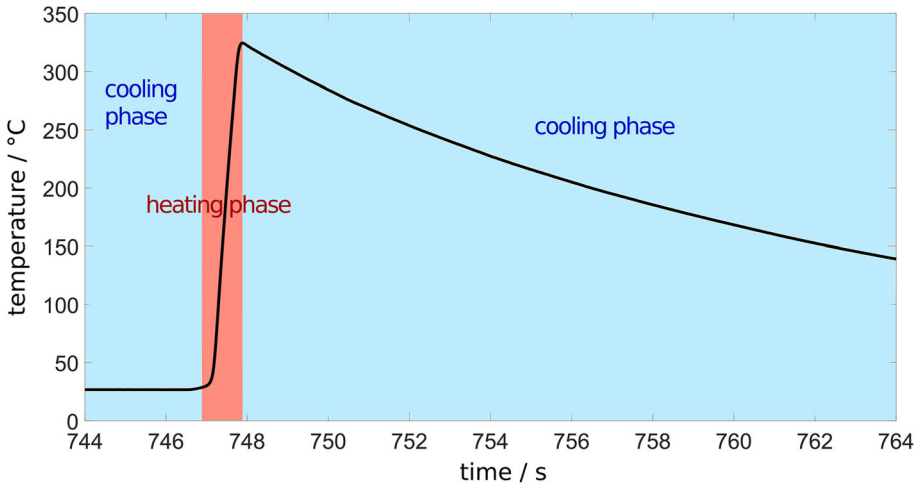

Fig. 3 Temperature curve during a singular PTP measurement. (F4MB-XL, flow 40 slm Ar + 4 slm H_2, current 600 A, axial distance 120 mm)

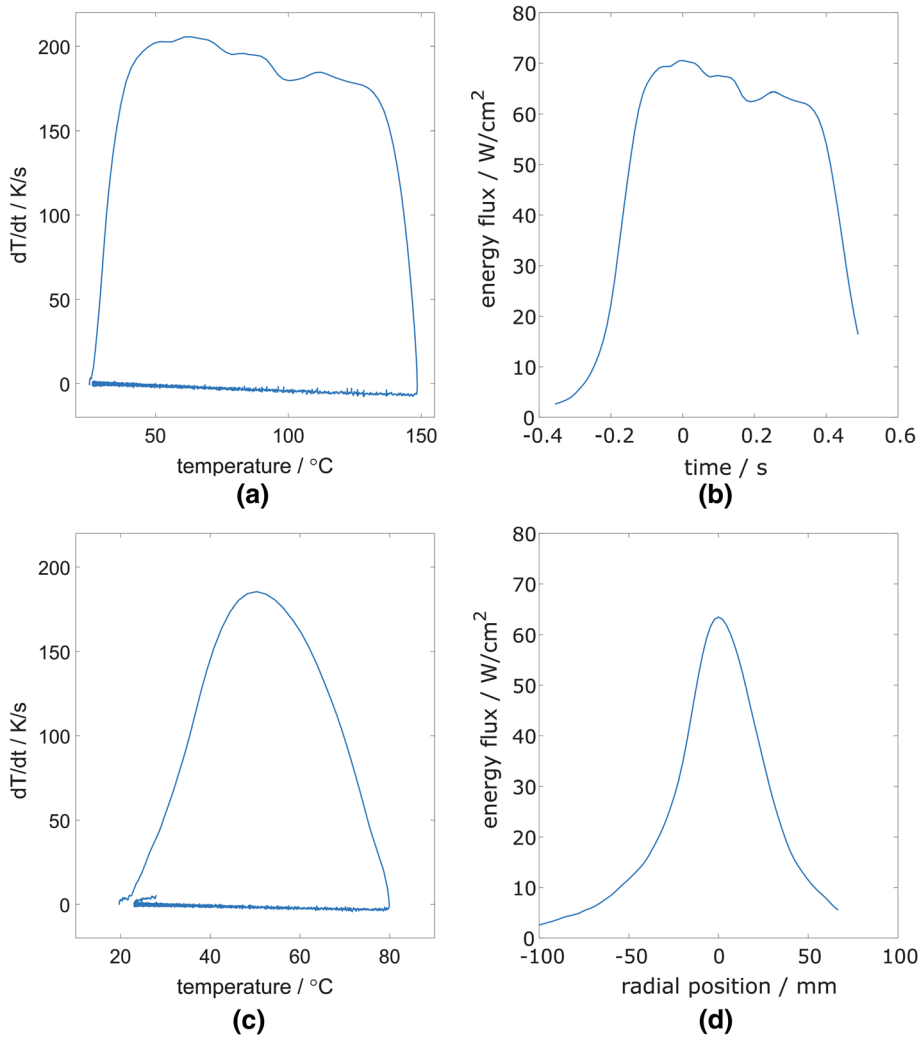

Fig. 4 (a) Depiction of dT/dt and (b) resulting temporal evolution of the energy flux using the established method for a resting jet of about 0.5 s. (c) Depiction of dT/dt and (d) resulting radial profile of the energy flux using the time-resolved evaluation method. (F4MB-XL, flow 40 slm Ar, current 600 A, axial distance 120 mm)

jet is continuously moved across the whole probe with constant velocity. That procedure results in a time- and, thus, position-dependent, inconstant energy flux. Figure 4(c) shows the dT/dt depiction of this procedure. The recorded time and constant velocity of the jet allow the calculation of the energy flux in dependence on the radial position of the probe relative to the centre of the jet under the assumption that the maximum energy flux is present in the jet centre. Such a radial profile is shown in Fig. 4(d). For comparison, Fig. 4(b) shows the time-dependent energy flux of the established method with a stationery time of 0.5 s where the energy flux is almost constant.

The experiments resulting in Fig. 4(b) and (d) respectively were performed under the same conditions. The average energy flux in Fig. 4(b) is 66 W/cm^2, the energy flux in the centre of Fig. 4(d) is 63.5 W/cm^2. They show a good agreement with a difference below 5%. In comparison, the radial profiles of the time-resolved method provide additional information, which can only be deduced by multiple measurements from the established method. Besides analysing the actual shape, it is possible to determine the width of the profile and its integrate. The integrate can be used to extrapolate the total deposited energy onto a substrate area larger than the probe itself since the entire profile is considered.

The plasma source InoCoat developed by the Co. INOCON Technologie GmbH, Attnang-Puchheim, Austria is a DC-based plasma spraying source with a maximum input power of 12 kW. To achieve a stable plasma an Ar flow between 5 slm and 20 slm is used. Additionally, hydrogen as molecular gas can be added to increase energy flux towards the substrate like in other commercial sources (Ref 33). The injection of coating material is done radially, thus, probably leading to an inhomogeneous powder distribution as described by Kavka et al. (Ref 34). The jet itself is mounted on a robotic arm to enable free spatial movement. The precise and reproducible movement of the jet is crucial for a homogeneous coating and measurements with PTPs alike. A single PTP is placed in a horizontal guide plate (25 × 17 cm) in an axial distance of 50 mm

(Fig. 5 a). For the energy flux measurement, the jet is moved with a velocity of 100 mm/s across the probe as described beforehand.

The second plasma spraying system studied is the F4MB-XL available from OC Oerlikon Management AG, Pfäffikon, Switzerland. It utilizes a DC arc as well but with a much higher input power of up to 55 kW. Thus, a direct comparison is not suitable. Ar is used as main process gas with a flow of up to 100 slm with an optional addition of the molecular gases hydrogen or nitrogen. Again, a robotic arm enables free spatial movement across a passive thermal probe mounted in a slightly larger guide plate (30 × 40 cm), see Fig. 5(b). Side-mounted air nozzles are optionally used for substrate cooling and changing the shape of the effluent. The axial distance is usually kept constant at 120 mm as typical coating distance and the jet is moved with a velocity of 200 mm/s.

Results and Discussion

Electrical Power and Molecular Gases

The electrical input power is one of the main process parameters for control of the deposition properties. A higher electrical power increases the energy density of the plasma as heat source for the melting of the deposition material. Thus, an adjustment of electrical power has a profound effect on the temperature distribution of particles and their degree of melting. On the other hand, this changes the temperature load of the substrate which can become critical when dealing with heat sensitive materials, e.g., polymers.

Figure 6 shows the changing energy flux with only Ar as process gas (black crosses) in dependence on the electrical power increasing from 8 to 34 kW with F4MB torch. It has to be mentioned that the device is not power- but current-regulated, i.e., the setpoint for the current is chosen manually and the applied voltage is adjusted accordingly. This regime leads to slight fluctuations of the power and, hence,

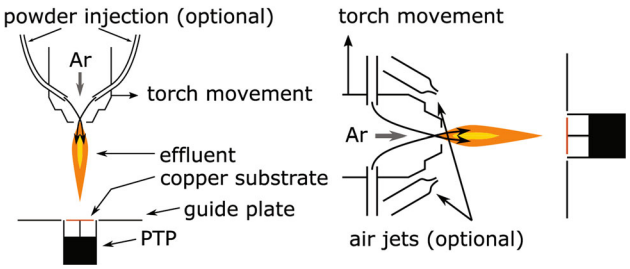

Fig. 5 Schematic layout of the experimental setup of the (a) InoCoat source with optional powder injection for deposition and of the (b) F4MB-XL source with optional air nozzles for manipulation of the shape of the effluent

a restricted reproducibility for the same current. The electrical power is simply calculated by multiplying the current and voltage.

The evaluation of electrical power and energy flux shows a distinct linear dependence. Therefore, a linear fit is conducted. This result shows a good agreement with similar investigations of a hot plasma jet done by Kewitz et al. (Ref 24). To investigate the influence of additional molecular gases different flows of hydrogen and nitrogen are added. The flows are in the range of 2-14 slm H_2 and 2-10 slm N_2. The value of the arc current intensity during these measurements is always 600 A. However, an increasing flow of additional molecular gas increases the voltage, thus, increasing the electrical power simultaneously. For that reason, these results are displayed over the power axis in Fig. 6 as well. The measured energy flux increases linearly similar to pure Ar but with a greater slope of (5.9 ± 1.1) W/cm^2/kW for H_2 and (4.5 ± 1.0) W/cm^2/kW for N_2 compared to (3.3 ± 0.2) W/cm^2/kW for Ar. At the same electrical power, e.g., 30 kW, the energy flux of both molecular gases is significantly higher compared to pure Ar. This is related to the increased thermal conductivity of mixtures of Ar with molecular gases (see e.g. Ref 35). The effect is associated also with the released binding energy when dissociated hydrogen or nitrogen atoms recombine with molecules on the substrate surface. Comparing the two molecular gases, H_2 generates a higher energy flux than N_2 at the same electrical power. A possible reason for that is the difference in dissociation energy. Hydrogen has a much lower binding energy of 4.5 eV per molecule than nitrogen (8.7 eV). Thus, hydrogen is more likely to get dissociated and recombined in the process.

Axial Distance

The (axial) distance between the plasma jet and the substrate (probe) is an important and crucial parameter to handle thermal load on the substrate, control layer formation and resulting film properties as well as changing the coating area. At a fixed current of 600 A the distance is varied from 160 mm to the minimal feasible distance using the time-resolved evaluation method. Since the energy flux increases considerably this minimal distance is dependent on gas mixture and represents the limitation of the temperature measurement. The upper limit for probes in the current study is reached for an energy flux of about 1500 W/cm^2, thus, the minimal distances are 10 mm for 40 slm Ar and 40 mm for additional 10 slm H_2 or N_2.

The energy flux in Fig. 7 shows a strong decrease with increasing distance. Addition of 10 slm H_2 or N_2 shows an increased energy flux at each distance. The course can be interpolated in good agreement with a square fit and is marked as well. With such quadratic function taken as a

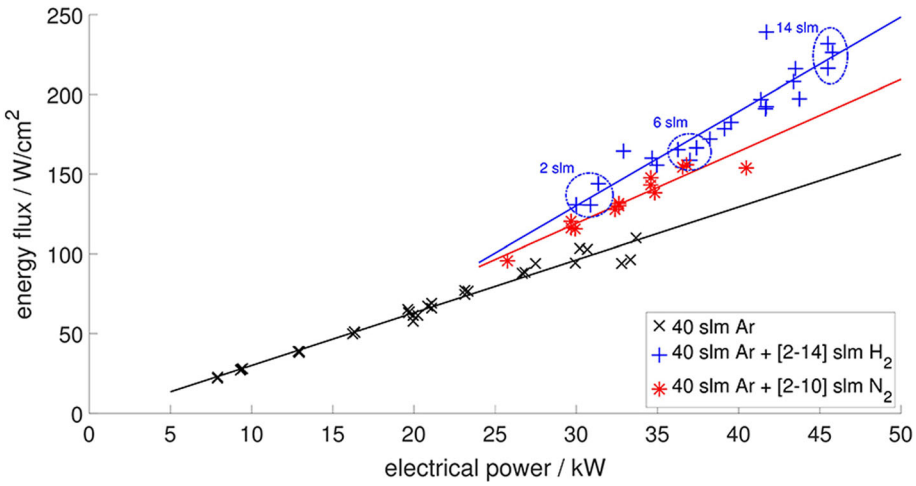

Fig. 6 Energy flux for an argon base plasma (40 slm) vs. variation of electrical power. For diatomic gases current is fixed at 600 A

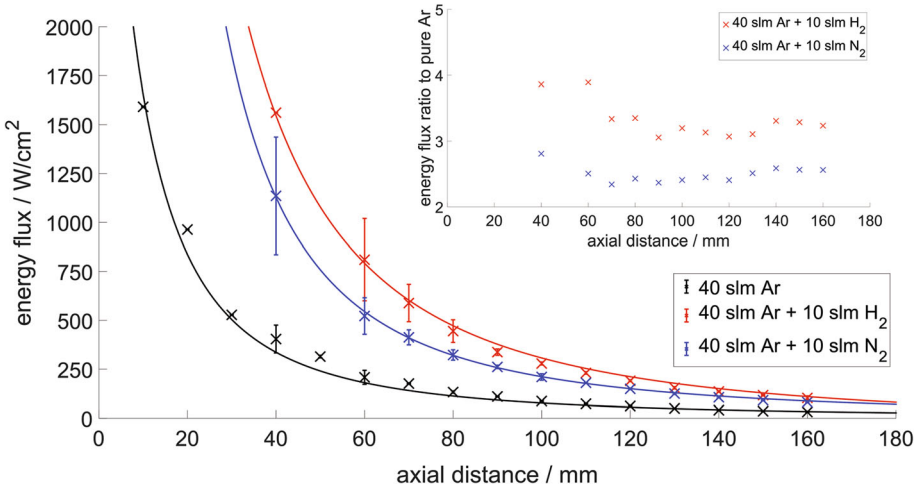

Fig. 7 Energy flux at 40 slm Ar flow with and without H_2 and N_2 for variation of the axial distance. Inset shows ratio of energy fluxes for H_2 and N_2 to pure Ar

basis it can be assumed that the energy flux distribution is cone-shaped with the jet as its origin. In other words, the same power is spread over an area which increases quadratically with the distance, thus, the measured energy flux density decreases accordingly (Ref 24). The inset in Fig. 7 depicts the energy flux ratios of added H_2 and N_2 compared to pure Ar. The ratios are slightly higher for low distances but are almost constant for distances above 60 mm. An increased ratio suggests an additional transport mechanism for energy at lower distances. A possible mechanism could be the recombination of molecules which should occur predominantly in close vicinity to the jet.

The variation of axial distance allows for a comparison with the results of Hugot et al. (Ref 21) which measured the thermal flux of a similar jet with a distance of 100 mm, current of 600 A and gas mixture of 36 slm Ar and 12 slm H_2. The maximum thermal, i.e., energy, flux they found in the centre of the plume is about 185 W/cm^2. The energy flux at a distance of 100 mm and additional H_2 in this work is about 280 W/cm^2. Besides the slightly different parameters and jet models, the sizes of the PTP in this work and the Medtherm 64 sensor used by Hugot et al. could explain the difference. Because the obtained energy flux values are an average value of the whole sensor area a smaller sensor would measure a higher energy flux in the centre of the jet due to the strong decrease in energy flux for remote radial distances. If the Medtherm 64 sensor has a sensor face which is considerably larger than the PTP´s diameter of 5.2 mm it would measure a lower energy flux under the same conditions.

As the measurements in Fig. 7 were performed using the time-resolved evaluation method discussed in section "Experimental Setup", the associated calculated radial profiles can be analysed likewise. The full with half maximum (FWHM) of the radial profiles is displayed in Fig. 8. The distance between the radial positions left and right of the centre where the energy flux is as close as possible to half the maximum value is used for FWHM. This additional information reveals a linear increase of the FWHM for all gas mixtures. This result confirms the assumption of a cone-shaped energy flux distribution because a linearly increasing diameter matches a quadratically increasing

area. Furthermore, the addition of molecular gases reduces the FWHM only to minor degree.

Radial Profile

A further investigation of the radial profiles was done in order to support the validity of the time-resolved evaluation method. Figure 9 depicts the energy flux of nine repeated measurements using this method compared with the established method which was performed at different radial positions. The good agreement approves the validity of the new method. The radial dependence shows a rapidly decreasing energy flux from the centre (about 60 W/cm^2) to remote radial positions. This corroborates the results of Selvan et al. (Ref 20) because their radial profiles show the same shape despite simulating a non-identical plasma source. They calculated a thermal flux of about 150 W/cm^2 in the centre for an identical arc current of 600 A but a smaller axial distance of 8 cm and different gas mixture (25 slm Ar and 3 slm N_2). These differences would result in a higher thermal flux in comparison to the parameters used for Fig. 9 and could explain the difference at least partially.

Chen et al. (Ref 15) used optical emission spectroscopy and an enthalpy probe to measure the temperature distribution of a comparable plasma jet. These radial temperature distributions resemble this characteristic shape as well. Since it is expected that the high gas temperature is one of the main energy flux contributions, the radial energy flux and radial temperature distributions seem to be correlated directly.

The radial distribution of energy flux is utilized for the characterization with injected powder material also. Figure 10 shows the radial energy flux distribution of the InoCoat source under industrial parameters for the deposition of a wear-resistant zinc layer. The investigation of the effect of coating material consists of two separate iterations. One without adding the zinc powder and one with additional powder. This procedure allows to analyse the influence of the powder directly because any change in energy flux is caused by the coating material. An increase in the energy flux is clearly visible in the centre of the jet but not at the edges below −20 mm or above 20 mm (Fig. 10). This indicates that the hot, molten zinc particles are primarily present in the centre of the effluent. The shape of two separate maxima could be observed when injecting the zinc particles. It suggests that the different shape is related to the radial insertion of the powder with a mean particle size of 30 µm from two opposing directions. It was already reported that these circumstances can lead to an asymmetrical material distribution (Ref 34). Due to the additional layer being very thin compared to the copper substrate of the probe, no change in heat capacity could be

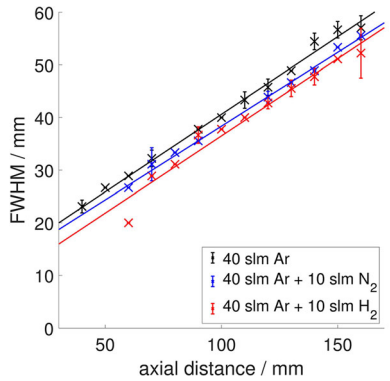

Fig. 8 Full with half maximum (FWHM) of radial energy flux profiles from measurements performed in Fig. 7

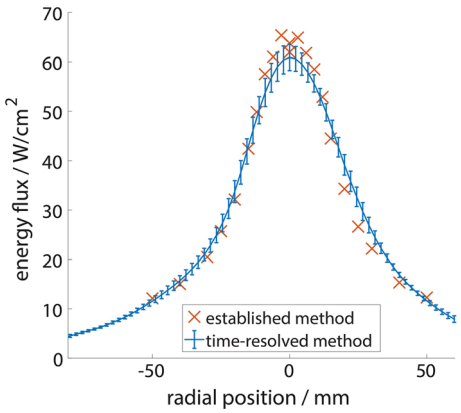

Fig. 9 Radial energy flux distribution of the F4MB-XL for established and time-resolved method. (F4MB-XL, flow 40 slm Ar, current 600 A, axial distance 120 mm)

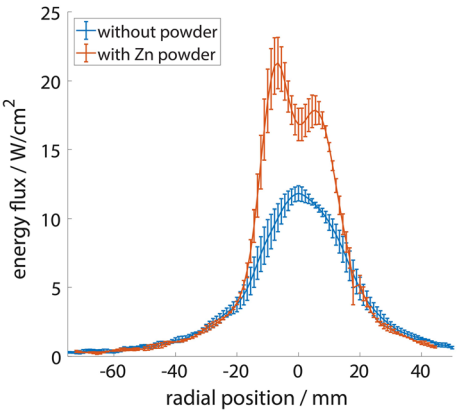

Fig. 10 Comparison of the radial energy flux distribution with and without the addition of Zn powder as precursor for spray coating. (InoCoat, flow 10 slm Ar, current < 100 A, axial distance 50 mm, powder rate 6 g/min)

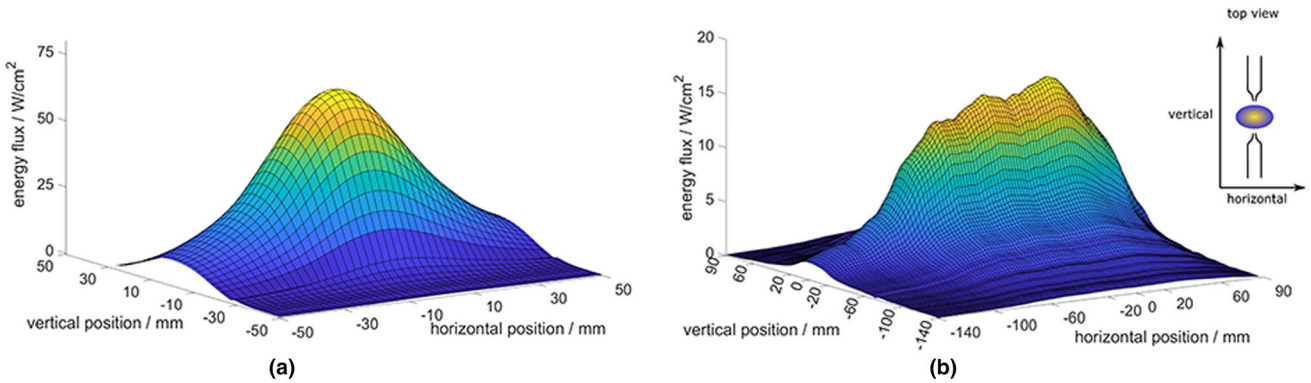

Fig. 11 2-D energy flux distribution when using external nozzles with compressed air. The air stream in (a) is parallel to the effluent, in (b) the air stream is focused on the position of the PTP. Inset shows geometry of air jets and energy flux distribution. (F4MB-XL, flow 40 slm Ar, current 600 A, axial distance 120 mm, air pressure 2 bar)

determined afterwards. The application of PTPs is proposed as a reliable diagnostic to evaluate the spatial distribution of coating material from the substrate perspective.

Profile Tailoring

For the purpose of testing further potential applications of the advanced time-resolved evaluation method, two-dimensional studies were performed. This characterization exploits the spatial information of two separate measuring passes. By changing the path of the jet movement across the probe, different axis of the energy flux can be incorporated. In this case, one horizontal and one vertical path is chosen. This allows for the calculation of a 2-D profile. To illustrate a change in the jet profile, two side-mounted air nozzles are used. They make it possible to manually change the shape of the effluent and are usually used for substrate cooling. Figure 11 displays the integrated 2-D profile jet profile for two different air nozzle positions at an air pressure of 2 bar. The first position in Fig. 11(a) is almost parallel to the jet direction, the second one in Fig. 11(b) is focused on the substrate surface at a distance of 120 mm. A parallel orientation of the air nozzles seems to have a minor influence on the shape as the profile is still similar to a rotationally symmetrical course of a 1-D profile in Fig. 9. The other depiction, however, shows a severe deformation. The profile is broadened and resembles a mountain ridge. Related to the deposition process this implies a coverage of a wider area at the same energy flux, hence, reducing the inhomogeneity on the substrate.

In addition, the deposited power can be derived by integrating the 2D profiles over the area. For a quadratic area with a side length of 400 mm around the centres in Fig. 11, the deposited powers are $P_{(a)} = 1.44$ kW and $P_{(b)} = 1.73$ kW respectively. For an electrical input power of about 20 kW that suggests an efficiency of about 8%. This exemplary measurement emphasizes the power of this diagnostics to provide a detailed understanding of the deposition conditions from the point of view of the substrate with a short measurement time of about 5 min.

Conclusions and Outlook

This study shows the applicability of passive thermal probes for the characterisation of high-power plasma spraying jets under atmospheric pressure. The capability to measure the energy flux from the point of view of an ordinary substrate provides insight into the interaction between the plasma source and substrate surface. The newly time-resolved evaluation method supplies additional spatial information about the process. The calorimetric measurements show a linear dependency of the energy flux on the electrical power. Compared to pure argon plasma, the addition of molecular gases results in steeper slopes, suggesting a more efficient energy transport. A cone-shaped spatial distribution is present for most parameters and not altered by adding molecular gases. Measurements with coating material should reveal the spatial distribution of the powder in the effluent. Moreover, two-dimensional spatial profiles are used to illustrate the influence of external air nozzles. When correlated with other diagnostics, e.g., thin film analysis, optical methods, passive thermal probes could be used as versatile and powerful diagnostic also for plasma spraying.

Acknowledgments The authors thank Dr. Jürgen M. Lackner, Dr. Alexander M. Schwan and Simon Chwatal from JOANNEUM RESEARCH Forschungsgesellschaft mbH for enabling the cooperation with INOCON Technologie GmbH. Furthermore, the authors thank Frank Brach, Daniel Köpp, Jens Zöllner-Krumme and the central workshop, physics centre, Kiel University for designing and building the setups and probes. Luka Hansen would like to thank the German Research Foundation (DFG, Project No. 413664940, Grant No. KE 574/8-1) for funding. Thorben Kewitz, Holger Testrich, and Rüdiger Foest are thankful for funding from the European Union and

the Federal State of Germany Mecklenburg-Western Pomerania (Project number TBI-V-1-321-VBW-112).

Funding Open Access funding enabled and organized by Projekt DEAL.

References

1. P. Fauchais, Understanding Plasma Spraying, *J.Phys. D: Appl. Phys.*, 2004, **37**(9), p R86-R108. https://doi.org/10.1088/0022-3727/37/9/R02
2. A. Vardelle, C. Moreau, N.J. Themelis and C. Chazelas, A Perspective on Plasma Spray Technology, *Plasma Chem. Plasma Process*, 2015, **35**(3), p 491-509. https://doi.org/10.1007/S11090-014-9600-Y/FIGURES/7
3. D.L. Ruckle, Plasma-Sprayed Ceramic Thermal Barrier Coatings for Turbine Vane Platforms, *Thin Solid Films*, 1980, **73**(2), p 455-461.
4. R.A. Miller, Current Status of Thermal Barrier Coatings — An Overview, *Surf. Coat. Technol.*, 1987, **30**(1), p 1-11.
5. R. Vaßen, H. Kaßner, A. Stuke, F. Hauler, D. Hathiramani and D. Stöver, Advanced Thermal Spray Technologies for Applications in Energy Systems, *Surf. Coat. Technol*, 2008, **202**(18), p 4432-4437.
6. G. Mauer and R. Vaßen, Current Developments and Challenges in Thermal Barrier Coatings, *Surf. Eng.*, 2011, **27**(7), p 477-479.
7. H. Singh, B.S. Sidhu, D. Puri and S. Prakash, Use of Plasma Spray Technology for Deposition of High Temperature Oxidation/Corrosion Resistant Coatings – a Review, *Mater. Corros.*, 2007, **58**(2), p 92-102. https://doi.org/10.1002/MACO.200603985
8. R.W. Smith and Z.Z. Mutasim, Reactive Plasma Spraying of Wear-Resistant Coatings, *J. Thermal Spray Technol.*, 1992, **1**(1), p 57-63. https://doi.org/10.1007/BF02657018
9. E. Lugscheider, Th. Weber, M. Knepper and F. Vizethum, Production of Biocompatible Coatings by Atmospheric Plasma Spraying, *Mater. Sci. Eng.: A*, 1991, **139**, p 45-48. https://doi.org/10.1016/0921-5093(91)90594-D
10. K. Landes, Diagnostics in Plasma Spraying Techniques, *Surf. Coat. Technol.*, 2006, **201**(5), p 1948-1954.
11. I.P. Gulyaev, M.P. Golubev, V.I. Kuzmin and P.A. Tyryshkin, Optical Study of Supersonic Jet Structure in Atmospheric Plasma Spraying, *AIP Conf. Proceed.*, 2018, **2027**(1), p 030066. https://doi.org/10.1063/1.5065160
12. J. Vattulainen, E. Hämäläinen, R. Hernberg, P. Vuoristo and T. Mäntylä, Novel Method for In-Flight Particle Temperature and Velocity Measurements in Plasma Spraying Using a Single CCD Camera, *J. Thermal Spray Technol.*, 2001, **10**(1), p 94-104. https://doi.org/10.1361/105996301770349556
13. J.F. Coudert, Michel Vardelle and Pierre Fauchais, DIAGNOSTICS OF PLASMA SPRAY PROCESS AND DERIVED ON-LINE CONTROL, *High Temp. Mater. Process (An Inter Quarterly High-Technol. Plasma Process.)*, 2002, **6**(2), p 19. https://doi.org/10.1615/HighTempMatProc.v6.i2.110
14. J. Schein, M. Richter, K.D. Landes, G. Forster, J. Zierhut and M. Dzulko, Tomographic Investigation of Plasma Jets Produced by Multielectrode Plasma Torches, *J. Therm. Spray Technol.*, 2008, **17**(3), p 338-343.
15. W.L.T. Chen, J. Heberlein and E. Pfender, Diagnostics of a Thermal Plasma Jet by Optical Emission Spectroscopy and Enthalpy Probe Measurements, *Plasma Chem Plasma Process*, 1994, **14**(3), p 317-332. https://doi.org/10.1007/BF01447084
16. Mohamed Rahmane, Gervais Soucy and Maher I. Boulos, Analysis of the Enthalpy Probe Technique for Thermal Plasma Diagnostics, *Rev. Sci. Instrument.*, 1995, **66**(6), p 3424-3431. https://doi.org/10.1063/1.1145517
17. C. Escure, M. Vardelle and P. Fauchais, Experimental and Theoretical Study of the Impact of Alumina Droplets on Cold and Hot Substrates, *Plasma Chem. Plasma Process.*, 2003, **23**(2), p 185-221. https://doi.org/10.1023/A:1022976914185
18. A. Vardelle, M. Vardelle, H. Zhang, N.J. Themelis and K. Gross, Volatilization of Metal Powders in Plasma Sprays, *J. Therm. Spray Technol.*, 2002, **11**(2), p 244-252. https://doi.org/10.1361/105996302770348907
19. G. Mauer, R. Vaen and D. Stöver, Plasma and Particle Temperature Measurements in Thermal Spray: Approaches and Applications, *J. Therm. Spray Technol.*, 2011, **20**(3), p 391-406.
20. B. Selvan, K. Ramachandran, B.C. Pillai and D. Subhakar, Numerical Modelling of Ar-N 2 Plasma Jet Impinging on a Flat Substrate, *J. Therm. Spray Technol.*, 2011, **20**(3), p 534-548.
21. F. Hugot, J. Patru, P. Fauchais and L. Bianchi, Modeling of a Substrate Thermomechanical Behavior during Plasma Spraying, *J. Mater. Process. Technol.*, 2007, **190**(1–3), p 317-323.
22. H. Kersten, H. Deutsch, H. Steffen, G.M.W. Kroesen and R. Hippler, The Energy Balance at Substrate Surfaces during Plasma Processing, *Vacuum, Pergamon*, 2001, **63**(3), p 385-431.
23. J. Benedikt, H. Kersten and A. Piel, Foundations of Measurement of Electrons, Ions and Species Fluxes toward Surfaces in Low-Temperature Plasmas, *Plasma Sources Sci. Technol.*, 2021, **30**(3), p 033001. https://doi.org/10.1088/1361-6595/abe4bf
24. T. Kewitz, M. Frohlich, J. von Frieling and H. Kersten, Investigation of a Commercial Atmospheric Pressure Plasma Jet by a Newly Designed Calorimetric Probe, *IEEE Transact. Plasma Sci.*, 2015, **43**(5), p 1769-1773. https://doi.org/10.1109/TPS.2015.2420679
25. T. Kewitz, M. Fröhlich and H. Kersten, Analysis of Passive Calorimetric Probe Measurements at High Energy Influxes, *EPJ Tech. Instrum.*, 2017, **4**(1), p 1-9. https://doi.org/10.1140/EPJTI/S40485-016-0036-Z
26. L. Hansen, K. Reck and H. Kersten, Energy Flux Measurements on an Atmospheric Pressure Surface Barrier Discharge, *J. Phys. D: Appl. Phys.*, 2019, **52**(32), p 325201. https://doi.org/10.1088/1361-6463/ab216c
27. L. Hansen, B. M. Goldberg, D. Feng, R. B. Miles, H. Kersten and S. Reuter, Energy Transfer in Interaction of a Cold Atmospheric Pressure Plasma Jet with Substrates, *Plasma Sources Sci. Technol.*, 2021, **30**(4), p 045004. https://doi.org/10.1088/1361-6595/abe955

28. L. Hansen, L. Rosenfeldt, K. A. Reck and H. Kersten, Understanding the Energy Balance of a Surface Barrier Discharge for Various Molecular Gases by a Multi-Diagnostic Approach, *J Appl. Phys.*, 2021, **129**(5), p 053308. https://doi.org/10.1063/5.0035671
29. S. Janisson, A. Vardelle, J.F. Coudert, E. Meillot, B. Pateyron and P. Fauchais, Plasma Spraying Using Ar-He-H2 Gas Mixtures, *J. Therm. Spray Technol.*, 1999, **8**(4), p 545-552. https://doi.org/10.1361/105996399770350232
30. S. Gauter, F. Haase and H. Kersten, Experimentally Unraveling the Energy Flux Originating from a DC Magnetron Sputtering Source, *Thin Solid Films*, 2019, **669**, p 8-18.
31. S. Bornholdt, J. Ye, S. Ulrich and H. Kersten, Energy Fluxes in a Radio-Frequency Magnetron Discharge for the Deposition of Superhard Cubic Boron Nitride Coatings, *J. Appl. Phys.*, 2012, **112**(12), p 123301. https://doi.org/10.1063/1.4769800
32. Lukas Rosenfeldt, Luka Hansen and Holger Kersten, The Use of Passive Thermal Probes for the Determination of Energy Fluxes in Atmospheric Pressure Plasmas, *IEEE Transact. Plasma Sci*, 2021, **49**(11), p 3325-3335. https://doi.org/10.1109/TPS.2021.3092752
33. A. Dolmaire, E. Hartikainen, S. Goutier, E. Béchade, M. Vardelle, P.M. Geffroy and A. Joulia, Benefits of Hydrogen in a Segmented-Anode Plasma Torch in Suspension Plasma Spraying, *J.Therm. Spray Technol.*, 2021, **30**(1–2), p 236-250. https://doi.org/10.1007/S11666-020-01134-2/FIGURES/17
34. T. Kavka, A. Maslani, J. Arnold and R. Henne, Influence of Injection Mode on Properties of DC Plasma Jets for Thermal Plasma Spraying, *Czechoslovak J. Phys*, 2004, **54**(3), p C766-C771. https://doi.org/10.1007/BF03166484
35. A.B. Murphy, "Transport Coefficients of Hydrogen and Argon-Hydrogen Plasmas," Plasma Chemistry and Plasma Processing, 2000.